The reaction of ethylene on a model automotive emissions control catalyst

R.M. Ferrizz [a], T. Egami [b] and J.M. Vohs [a]

[a] *Department of Chemical Engineering, University of Pennsylvania, Philadelphia, PA 19104, USA*
[b] *Department of Materials Science and Engineering, University of Pennsylvania, Philadelphia, PA 19104, USA*

Received 22 February 1999; accepted 2 June 1999

The reaction of ethylene on a model automotive emissions control catalyst consisting of Rh particles on an epitaxial ceria film grown on the (100) surface of an yttria-stabilized zirconia single crystal was studied using TPD. The TPD results showed that ethylene undergoes dehydrogenation on the model catalyst at temperatures below 500 K depositing carbon on the Rh particles. Surface carbon formed in this manner was oxidized to CO upon heating to above 550 K using oxygen supplied by the ceria lattice. Heating to 900 K was found to induce reduction of the ceria film resulting in a marked decrease in oxidation activity.

Keywords: ceria, emissions control, Rh, ethylene

1. Introduction

The oxidation of residual hydrocarbons is an important catalytic reaction in automotive emissions control. Current emissions control catalysts consist of a ceramic monolith coated with γ-alumina and impregnated with oxide promoters (CeO_2, ZrO_2, La_2O_3) and catalytic Group VIII metals (Rh, Pt, Pd). Ceria and zirconia are particularly important oxide components in this catalytic system. Ceria is known to perform several functions, including stabilization of the surface area of the support [1] and maintenance of the dispersion of the catalytic metals [2]. The most important role of ceria in this system, however, is to provide oxygen storage capacity [3–7]. The two stable oxidation states of cerium, Ce^{4+} and Ce^{3+}, allow ceria to either take up or release oxygen depending on whether the gas phase is fuel or oxygen rich. Addition of zirconia enhances the redox properties of ceria and results in higher oxygen storage capacity [4,8–10]. This oxygen storage capacity is vital in increasing the “operating window” of the air/fuel ratio over which sufficient oxidation activity can be maintained.

In a previous series of studies we have investigated the redox properties of ceria and the mechanism by which ceria provides oxygen for reaction with species adsorbed on the supported metals [3,4,11–13]. These studies have made use of model catalysts comprised of ceria single crystals and ceria thin films supported on sapphire and polycrystalline and single-crystalline zirconia. Our previous reactivity studies have focused exclusively on the oxidation of CO to CO_2. In the work presented here we have extended our previous studies to include the reaction of a hydrocarbon, ethylene, on a model automotive emissions control catalyst consisting of Rh supported on an epitaxial ceria film on an yttria-stabilized zirconia single crystal. The results of this study provide additional insight into the function of both ceria and zirconia in automotive emissions control catalysts.

2. Experimental

The model catalysts used in this study consisted of Rh particles supported on thin, epitaxial films of ceria grown on the (100) surface of an yttria-stabilized zirconia (YSZ) single crystal. Ceria film growth, Rh deposition, and TPD studies were all conducted in a single ultra-high vacuum surface analysis system. This system had a background pressure of 2×10^{-10} Torr and was equipped with a mass spectrometer (UTI), cylindrical mirror electron energy analyzer (Omicron), ion sputter gun (Physical Electronics), electron gun, quartz crystal film thickness monitor, and metal deposition sources.

The YSZ(100) substrate was cleaned via sputtering with 2 keV Ar^+ ions followed by annealing at 800 K for 60 min. This procedure was repeated until the surface was free from impurities as determined by Auger electron spectroscopy (AES). Ceria films were grown on the clean YSZ(100) substrate by vapor depositing cerium metal in the presence of 6×10^{-7} Torr of O_2. The cerium source consisted of a small tantalum boat filled with cerium metal, which could be heated by electron bombardment. Ceria films 10 monolayers ($\sim$40 Å) in thickness, as determined using the quartz crystal film thickness monitor, were used in this study. After deposition of the ceria layer, the film was annealed at 600 K in 6×10^{-7} Torr of O_2 for 1 h to ensure that the cerium was completely oxidized. In previous studies it was demonstrated that this growth procedure results in epitaxial ceria films that are oriented in the (100) direction [3,14].

The Rh metal source consisted of a small Rh wire wrapped around a tungsten filament which could be resis-

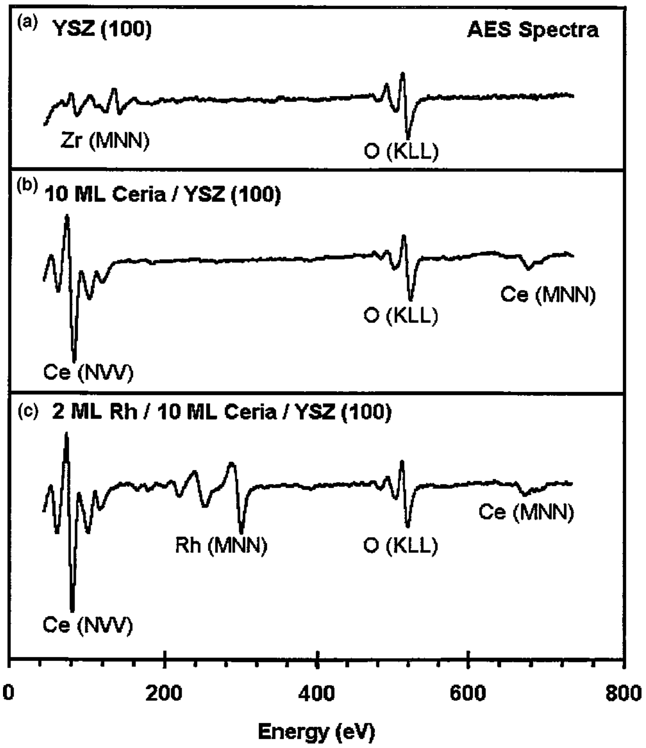

Figure 1. Auger spectra (2 keV beam energy) of (a) clean YSZ(100) surface, (b) epitaxial ceria thin film grown on YSZ(100), and (c) Rh particles deposited on the epitaxial ceria film.

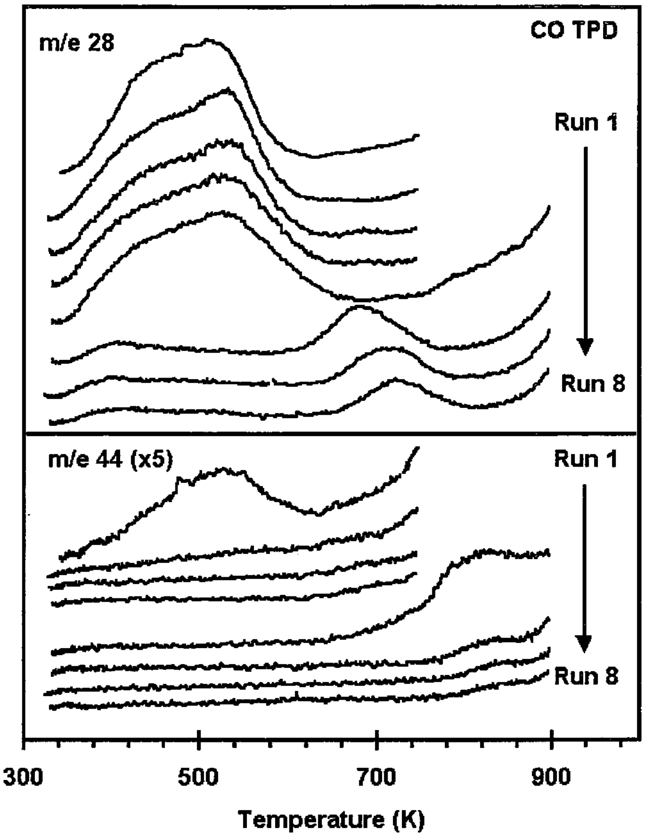

Figure 2. Series of CO TPD results obtained from a freshly prepared Rh/CeO$_2$/YSZ(100) sample. A CO exposure of 10 L was used in each run.

tively heated. An equivalent Rh coverage of two monolayers was used in this study. It has previously been demonstrated that Rh does not wet the surface of the ceria films and forms metal particles during deposition at 300 K [15,16].

AES was used to characterize the surface of the sample before and after ceria film growth and Rh deposition. AES spectra of the clean YSZ(100) substrate, the 10 ML ceria film and the Rh-covered ceria film are shown in figure 1. Note that peaks indicative of Zr are not present in the AES spectrum of the 10 ML ceria film. This result is consistent with previous studies and further demonstrates that the ceria film completely covers the surface of the YSZ substrate [4,14]. The lack of diminution of the Ce(NVV) peak upon Rh deposition is consistent with the formation of Rh particles.

Ethylene and CO were both obtained from Matheson and dosed on the surface of the sample via a variable leak valve equipped with a directional doser. The enhancement of the reactant flux to the sample due to the directional doser was estimated to be 10 times greater than that determined using the overall chamber pressure. Exposures quoted in this work have been corrected to reflect this enhancement factor. A heating rate of 4 K/s was used in all TPD experiments.

3. Results

In order to allow comparisons to the reactivity of the Rh/CeO$_2$/YSZ(100) samples used here with those in our earlier studies [3], CO TPD experiments were initially performed. A series of CO TPD spectra obtained from a freshly prepared Rh/CeO$_2$/YSZ(100) sample are displayed in figure 2. A room-temperature CO exposure of 10 L was used in all of the TPD runs in this series. In the first four runs, the temperature ramp was stopped at 750 K, while in subsequent runs, the sample was heated to 900 K. The only desorption products detected were CO (m/e 28) and CO$_2$ (m/e 44).

In the first TPD run, CO desorbed in a broad feature between 360 and 620 K, with the peak maximum occurring at 535 K. A smaller amount of CO$_2$ desorption was also detected over this same temperature range. A quantitative analysis of the data reveals that 18% of the adsorbed CO was oxidized to CO$_2$. These results are similar to those reported in our earlier studies [3], except that the amount of CO$_2$ produced is somewhat less.

In the second–fourth TPD runs, only the CO desorption feature was observed. In the fifth TPD run, the first in which the sample was heated to 900 K, the CO peak was similar to that in the earlier runs; however, a new high-temperature CO$_2$ peak was observed at 810 K. In our previous TPD studies of Rh/CeO$_2$/YSZ(100), the heating ramp was always stopped at temperatures below 800 K, thus this new high-temperature CO$_2$ peak was not observed. The origin of this peak has yet to be determined, but it may result from oxidation of carbon on the surface of the ceria film.

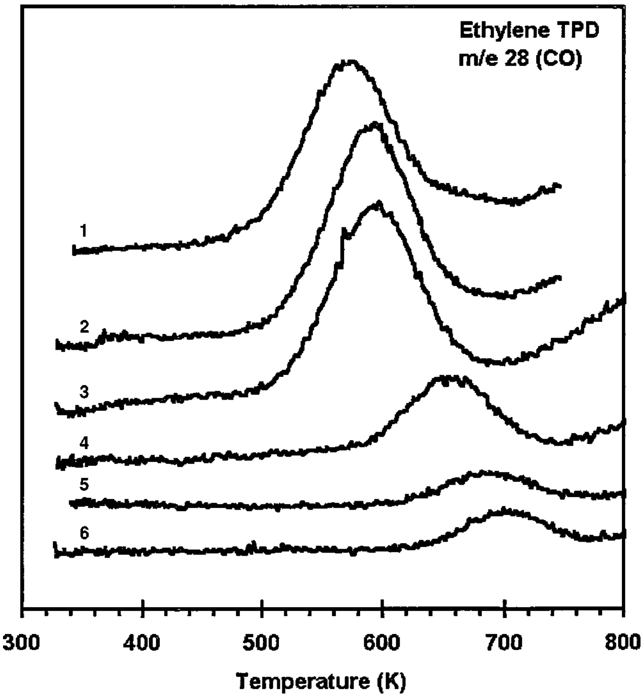

Figure 3. Series of m/e 28 (CO) TPD spectra obtained from an ethylene-dosed Rh/CeO_2/YSZ(100) sample. An ethylene exposure of 100 L was used in each run.

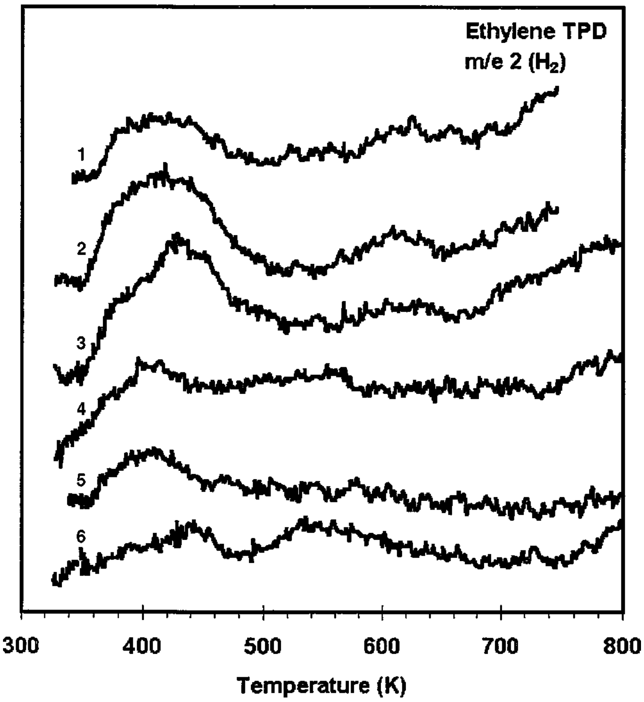

Figure 4. Series of m/e 2 (H_2) TPD spectra obtained from an ethylene-dosed Rh/CeO_2/YSZ(100) sample. An ethylene exposure of 100 L was used in each run.

Heating the sample to 900 K produced significant changes in the CO TPD results (see data for runs 6–8), the most noticeable being the absence of CO desorption between 360 and 620 K. This peak is replaced by a new CO peak centered at 690 K. The peak maximum of this feature was found to increase slightly with each TPD cycle. As demonstrated in our earlier studies using isotopically labeled CO [3,13], the peak near 700 K results from the oxidation of carbon atoms that are formed by dissociation of CO at lower temperature. This peak is only observed when the ceria film is highly reduced. This result, therefore, demonstrates that heating the sample to 900 K results in substantial reduction of the ceria film.

A series of ethylene TPD experiments were performed on a freshly prepared Rh/CeO_2/YSZ(100) sample. In runs 1 and 2 in this series, the sample was heated to 750 K, while in runs 3–6, the sample was heated to 900 K. The results of these experiments are presented in figures 3, 4, and 5, which display the m/e 28, 2, and 44 TPD spectra, respectively. The spectra for all other masses monitored, most notably m/e 27 and 18, did not exhibit any peaks.

The first ethylene TPD run (see run 1 in figures 3 and 4) contained both a m/e 28 peak at 570 K and a very broad H_2 (m/e 2) desorption feature centered at 400 K. Unfortunately, due to the relatively high background level of H_2 in the ion-pumped vacuum system, the data for H_2 desorption is rather noisy. It does appear, however, that there is an additional H_2 desorption peak centered at ~630 K. This result is similar to that reported by Dubois et al. for H_2 evolution during TPD from ethylene-dosed Rh(111) [17]. In that study, H_2 desorbed in a peak centered at 400 K which had a high-temperature tail that extended up to 750 K. Except for a rising signal at the end of the run which is due to desorption from the sample support hardware, the m/e 44

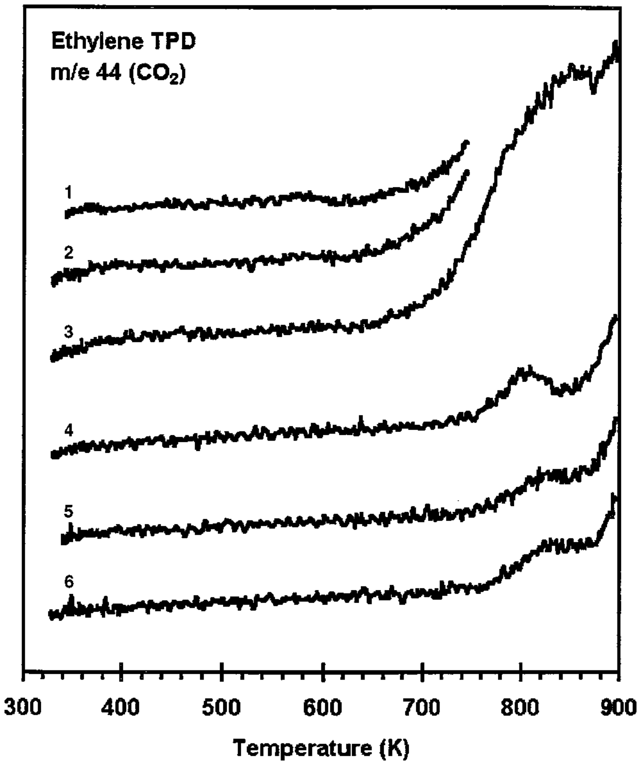

Figure 5. Series of m/e 44 (CO_2) TPD spectra obtained from an ethylene-dosed Rh/CeO_2/YSZ(100) sample. An ethylene exposure of 100 L was used in each run.

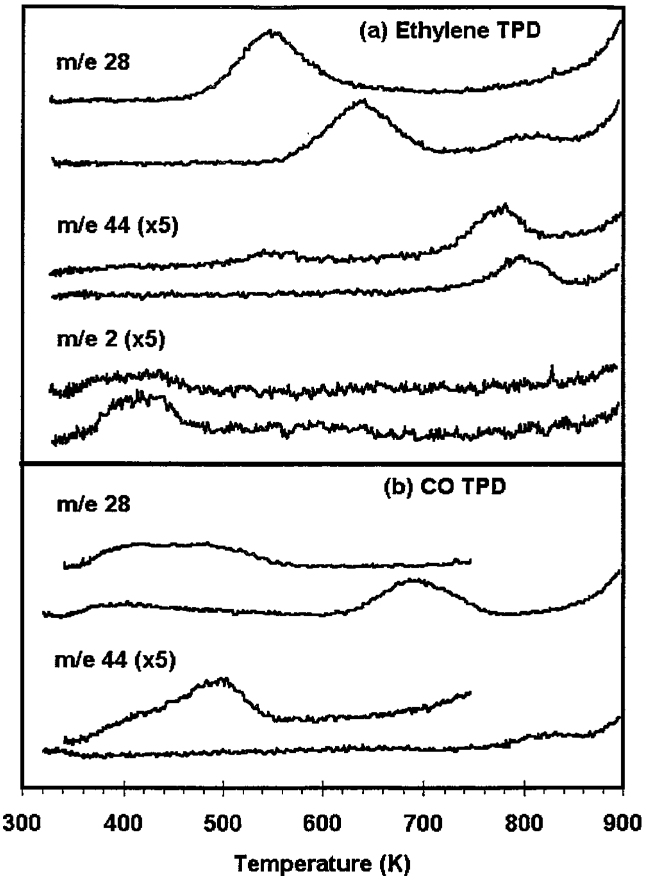

Figure 6. Ethylene and CO TPD data obtained from a re-oxidized Rh/CeO_2/YSZ(100) sample. (a) Mass 28, 2, and 44 spectra for 100 L, 300 K ethylene exposure. (b) Mass 28 and 44 spectra for 10 L, 300 K CO exposure. The top spectrum for each mass was obtained from the freshly re-oxidized sample, while the bottom spectrum was obtained after several TPD runs and is indicative of a reduced sample.

spectrum was flat. The TPD spectra for m/e 27, 26 and 25, which are present in the mass spectrometer cracking pattern of ethylene, did not exhibit any peaks. Therefore, the m/e 28 desorption feature at 570 K can be ascribed to CO.

The results of the second ethylene TPD run are similar to those of the first, except for a small decrease in the intensity of the CO and H_2 desorption features and a shift in the CO peak position from 570 to 600 K. The decrease in the intensity of the peaks is most likely due to a change in the morphology of the metal particles which occurred upon heating to 750 K. The third run was the first in which the sample was heated to 900 K. Both the m/e 28 and 2 spectra are almost identical to those in run 2; however, the m/e 44 spectrum contains a broad shoulder centered at roughly 800 K on the high-temperature, rising background. In subsequent runs this feature appeared as a distinct peak near 810 K.

As was the case for CO TPD, heating the sample to 900 K produced significant changes in the ethylene TPD results. The m/e 28 spectra for runs 4–6 exhibit a gradual increase in the CO desorption temperature along with a rapid decrease in the peak area. By run 6, CO desorbed at 700 K, and the peak area was reduced to approximately 15% of that in run 3. This decrease in the peak area can be attributed to sintering of the Rh film upon heating to 900 K. Note that a similar trend is observed in the CO TPD data. The shape of the H_2 desorption spectrum also changed significantly throughout the series. In the final run, H_2 desorbed in two peaks centered at 430 and 530 K.

To determine the reversibility of the changes observed in the TPD results that occurred upon heating to 900 K, experiments were also performed on reoxidized samples. The ceria films were reoxidized by annealing at 600 K for 1 h in a pressure of 6×10^{-7} Torr of O_2. CO and ethylene TPD results obtained from reoxidized samples are presented in figure 6. In both cases, the trends observed in the TPD results closely resemble those in the data from the freshly prepared samples.

4. Discussion

The interaction of ethylene with Rh has previously been studied in detail [17–23]. It has been shown that ethylene adsorbs dissociatively on Rh single crystals at room temperature. On Rh(100), ethylene reacts to form both CCH_3 (ethylidyne) and CCH. For coverages greater than 0.5 ML, ethylidyne predominates, while at lower coverages the CCH species predominates [22]. In contrast, on Rh(111), ethylene reacts at room temperature to form exclusively ethylidyne [17,19,20,23]. For Rh supported on alumina, ethylene also adsorbs dissociatively forming primarily ethylidyne, with smaller amounts of other hydrocarbon species [21]. Upon heating to approximately 400 K, adsorbed ethylidyne on Rh undergoes dehydrogenation forming CCH_2 and CCH [22]. These hydrocarbon fragments undergo further dehydrogenation over a broad temperature range (500–800 K), ultimately depositing carbon on the surface.

Based on the results obtained for Rh single crystals, one would expect ethylene to adsorb dissociatively at 300 K on the Rh/CeO_2/YSZ(100) samples studied in this investigation to form primarily ethylidyne, with progressive dehydrogenation occurring upon heating. The H_2 TPD spectra (see figure 4) obtained from ethylene-dosed Rh/CeO_2/YSZ(100) are indeed similar to those reported in the literature for the reaction of ethylene on Rh(111) [11,12,17,22] and are thus consistent with this scenario.

The TPD results displayed in figure 3 clearly demonstrate that, on Rh/CeO_2/YSZ(100), surface carbon formed by the dehydrogenation of ethylene can be oxidized to CO. The oxygen for this reaction must be supplied by reduction of the ceria support. During TPD using an oxidized ceria film this process results in a CO peak centered at 570 K. Note that this peak temperature is significantly greater than that for CO desorption from CO-dosed samples (see figure 2). This demonstrates that the CO peak at 570 K results from a reaction limited process. The rate-limiting step for this process can be either oxidation of the adsorbed carbon or the transfer of oxygen atoms from ceria to Rh. As shown in figure 2, oxidation of adsorbed CO to CO_2 using oxygen from the ceria lattice commences at temperatures below 500 K. This indicates that transfer of oxygen from the ceria to the Rh is relatively facile for a freshly grown ceria film. Thus, the CO peak at 570 K in the TPD results from the ethylene-dosed sample must be limited by the kinetics of the $C + O$ reaction. It is interesting that oxidation of surface carbon formed by dehydrogenation of ethylene results only in the production of CO and not CO_2. Apparently once CO is formed it desorbs before it can be further oxidized to CO_2.

The trends observed in the ethylene TPD series provide insight into changes in the oxidation activity of the model catalyst as a function of the extent of reduction of the ceria film. In the ethylene TPD results for the freshly prepared catalyst, CO desorbed in a peak centered at 570 K. Since the production of CO requires the removal of oxygen from the ceria film, each successive TPD run increases the extent of reduction of the ceria layer. As shown in runs 2 and 3 in figure 3, reduction of the ceria film produces an increase in the CO desorption temperature. In these runs the CO peak is centered at 590 K. This shift can be attributed to a gradual shift in the rate-limiting step from the kinetics of the surface reaction to transfer of oxygen from the ceria layer to the Rh.

As shown in runs 4–6 in figure 3, heating the $Rh/CeO_2/YSZ(100)$ model catalyst to 900 K produced a marked increase in the CO desorption temperature. In run 4, the first run after the sample had been heated to 900 K, the CO peak resulting from oxidation of adsorbed carbon is centered at 650 K, while in run 6 it appears at 700 K. This again demonstrates that the activation energy for transferring oxygen from the ceria film to the supported metal is a strong function of the extent of reduction of the ceria. It is interesting that similar trends are observed in the TPD results for the CO-dosed samples that had been heated to 900 K. As discussed above, CO dissociates on reduced $Rh/CeO_2/YSZ(100)$ at a relatively low temperature and the resulting surface carbon is reoxidized to CO at high temperature. Taken together, these results clearly show that heating to 900 K significantly reduces the ceria film. This conclusion is consistent with our previous TPD study of O_2 desorption from ceria single crystals and ceria supported on polycrystalline zirconia [11,12]. That study demonstrated that the desorption of O_2 from a zirconia-supported ceria thin film commenced at approximately 800 K. In contrast, O_2 desorption commenced at 1300 K from the ceria single crystal surface. The ability of the zirconia-supported ceria film to release oxygen at lower temperature is believed to be responsible for its enhanced oxidation activity.

Both the CO and C_2H_4 TPD results for reduced $Rh/CeO_2/YSZ(100)$ samples exhibit small CO_2 desorption peaks near 810 K. Although the origin of these peaks has yet to be unambiguously determined, it is unlikely that they result from oxidation of carbon deposited on the Rh, since this pathway would proceed through CO, which desorbs at lower temperature. Another possibility is that the CO_2 production results from the oxidation of C on the ceria rather than the metal. Although both CO and ethylene do not absorb on the surface of the ceria films in UHV, it is possible that a small fraction of the carbon atoms deposited on the metal diffuse onto the ceria support.

5. Conclusions

The results of this study demonstrate that ethylene adsorbs dissociatively on Rh sites on $Rh/CeO_2/YSZ(100)$ model catalysts at room temperature and then undergoes additional dehydrogenation upon heating. Surface carbon formed by this process is oxidized to CO at temperatures above 550 K. This result demonstrates that, like CO, hydrocarbons adsorbed on the supported Rh can be oxidized using oxygen supplied by reduction of the ceria film. Furthermore, the extent of reduction of the ceria layer plays an important role in determining the overall oxidation activity. As the ceria film becomes more reduced, the desorption temperature of the oxidation product, CO, increases substantially. For an oxidized film, CO production is apparently limited by the $C + O$ surface reaction, while for a more reduced film, CO production is limited by transfer of oxygen from the ceria film to the supported metal. These changes were found to be reversible and annealing in oxygen restored the activity of the system. The results of this study also provide additional evidence that ceria supported on zirconia is more easily reduced than bulk ceria. Heating to 900 K results in significant reduction of the zirconia-supported ceria, while heating to 1300 K is required to reduce bulk ceria.

Acknowledgement

This work was supported by the Department of Energy, Office of Basic Energy Sciences (grant no. DE-FG02-96ER14682). Some facilities used in this work were also partially funded by the National Science Foundation through the MRSEC program (grant no. DMR-963298).

References

[1] G. Kim, Ind. Eng. Chem. Prod. Res. Dev. 32 (1982) 73.
[2] J.C. Summers and S.A. Ausen, J. Catal. 58 (1979) 131.
[3] E.S. Putna, R.J. Gorte and J.M. Vohs, J. Catal. 178 (1998) 598.
[4] E.S. Putna, T. Bunluesin, X.L. Fan, R.J. Gorte and J.M. Vohs, Catal. Today, in press.
[5] K. Otsuka, M. Hatano and A. Morikawa, J. Catal. 79 (1983) 493.
[6] R.K. Herz and J.A. Sell, J. Catal. 94 (1985) 199.
[7] H.S. Gandhi and M. Shelef, Stud. Surf. Sci. Catal. 30 (1987) 199.
[8] M. Haneda, K. Miki, N. Katusa, A. Ueno, S. Tani, S. Matsuura and M. Sato, Nihon Kagaku Kaishi (1990) 820.
[9] T. Ohatu, Rare Earths 17 (1990) 37.
[10] T. Murota, T. Hasegawa, S. Aozasa, H. Matsui and M. Motoyama, J. Alloys Comp. 193 (1993) 298.

[11] E.S. Putna, J.M. Vohs and R.J. Gorte, J. Phys. Chem. 100 (1996) 17862.

[12] E.S. Putna, J.M. Vohs and R.J. Gorte, Catal. Lett. 45 (1997) 143.

[13] J. Stubenrauch and J.M. Vohs, Catal. Lett. 47 (1997) 21.

[14] W. Dmowski, T. Egami, R. Gorte and J. Vohs, Physica B 221 (1996) 420.

[15] J. Stubenrauch and J.M. Vohs, J. Catal. 159 (1996) 50.

[16] J. Stubenrauch, Ph.D. thesis, University of Pennsylvania (1997).

[17] L.H. Dubois, D.G. Castner and G.A. Somorjai, J. Chem. Phys. 72 (1980) 5234.

[18] M.J. Calhorda, P.E.M. Lopes and C.M. Friend, J. Mol. Catal. A 97 (1994) 157.

[19] B.E. Bent, C.M. Mate, C.T. Kao, A.J. Slavin and G.A. Somorjai, J. Phys. Chem. 92 (1988) 4720.

[20] B.E. Koel, B.E. Bent and G.A. Somorjai, Surf. Sci. 146 (1984) 211.

[21] T.P. Beebe and J.T. Yates, J. Phys. Chem. 91 (1987) 254.

[22] A.J. Slavin, B.E. Bent, C.T. Kao and G.A. Somorjai, Surf. Sci. 206 (1988) 124.

[23] R.J. Koestner, M.A.V. Hove and G.A. Somorjai, Surf. Sci. 121 (1982) 321.